Ground-State Energy of the Electron Liquid in Ultrathin Wires

Michael M. Fogler

Department of Physics, University of California San Diego, La Jolla, California 92093, USA

(Received 17 December 2004; published 10 February 2005)

The ground-state energy and the density correlation function of the electron liquid in a thin one-dimensional wire are computed. The calculation is based on an approximate mapping of the problem with a realistic Coulomb interaction law onto exactly solvable models of mathematical physics. This approach becomes asymptotically exact in the limit of a small wire radius but remains numerically accurate even for modestly thin wires.

DOI: 10.1103/PhysRevLett.94.056405 PACS numbers: 71.10.Pm, 73.21.Hb, 73.22.–f

Recently much attention has been devoted to a class of one-dimensional (1D) conductors that can be termed ultrathin wires. Examples of such systems include single-wall carbon nanotubes (CN) [1], semiconductor nanowires [2], and conducting molecules [3]. *Semiconducting* ultrathin wires are especially interesting because their electron concentration n can be varied by the field effect, which can be used for creating miniature electronic devices [4,5]. In such applications a fundamental role is played by the concentration dependence of the ground-state energy density $\varepsilon(n)$. This function determines the electrostatic screening and affects the capacitive coupling of the electron liquid to external voltage sources. It is also a core input of the density-functional theory (DFT), which is the basis of today's electronic structure calculations. Since the 3D Fermi-liquid theory does not hold in 1D, it is unclear whether the usual DFT optimized for three-dimensional (3D) systems is adequate for ultrathin wires. The Luttinger liquid (LL) theory [6], which is called upon to replace the Fermi-liquid theory, makes no predictions for the short-range physics that determines $\varepsilon(n)$. Therefore, the calculation of the ground-state energy of 1D wires with realistic Coulomb interactions has remained an open problem. The primary difficulty is the computation of the correlation energy $\varepsilon_{\rm cor}$, which is determined by the shape and size of the exchange-correlation hole (XCH), i.e., the reduction in probability of any two electrons closely approaching each other. Below we propose a theory that calculates these quantities.

Model.—Our calculation is done for an N-component electron gas, N being the combined spin-valley degeneracy of the electron spectrum. For example, $N = 4$ in CN [1]. The aforementioned XCH is the term that refers to the negative dip of the two-body cluster function $h(x)$ around $x = 0$. Here $h(x) = (Mn)^{-1}\sum_{i\neq j}\langle\delta(x_i - x_j - x)\rangle - 1$, M is the number of electrons, and x_i are their coordinates. Larger $|h(0)|$ imply stronger correlations. Since $\int_{-\infty}^{\infty} h(x)dx = -1/n$, the XCH has a characteristic width $l_* \sim 1/n|h(0)|$. For example, in the free Fermi gas $h(x) = -N\sin^2(nx/N)/n^2x^2$, so that $|h(0)| = 1/N$ and l_* is equal to N/n, the average distance among electrons of the same species or, as we call it, the same *isospin.* Our goal is to compute $h(x)$ for an interacting system. Once $h(x)$ is known, $\varepsilon(n)$ can be obtained straightforwardly; see below. We model the interactions by the potential $U(x) = e^2/\kappa\sqrt{x^2 + R^2}$, which accounts for smoothing of Coulomb repulsion at distances of the order of the wire radius R. The wire is considered ultrathin if the parameter $\mathcal{L} = \ln(a_B/R)$ is large, where $a_B = \hbar^2\kappa/me^2$, m, and κ are the effective Bohr radius, electron mass, and dielectric constant, respectively. On general grounds, we may expect that at low densities, $n \ll 1/a_B$, electrons should form a 1D Wigner "crystal" [7] with $h(x)$ sharply peaked at integer multiples of $a = 1/n$. At $n \gg 1/a_B$ where electrons have a large kinetic energy, $h(x)$ should remain appreciable down to $x \ll a$. Below we refine and flesh out this qualitative picture by quantitative calculations.

Crucial for our approach is the fact that to the leading order in $1/\mathcal{L}$ the problem in hand and the problem with the contact interaction, $U(x) = (\hbar^2 c/m)\delta(x)$, give the same short-range behavior of the correlation functions, including the XCH. Here c is given by

$$c = (2/a_B)\ln(l_*/R). \tag{1}$$

This remarkable mapping between the two interaction laws holds only in the liquid state, $n \gg 1/a_B$. The reason for it becomes clear if one carefully separates the effects of the sharp maximum ("core") of the Coulomb potential $U(x)$ at $x = 0$ from those of its $1/x$ tails. As was shown in our earlier work [8], the condition $n \gg 1/a_B$ guarantees that the Coulomb tails have negligible effects on $h(x)$ up to exponentially large distances, $\ln(x/a) \sim 1/r_s$, where $r_s = a/2a_B \ll 1$. Since r_s plays the role of the dimensionless coupling constant, this agrees with the conventional wisdom. On the other hand, the electron scattering caused by the short-range core of $U(x)$ is enhanced [8] by the large logarithm $\mathcal{L}$. Therefore, the Coulomb potential acts as a sum of a strong short-range core and weak tails, and so can be mapped onto a suitable δ function.

The rest of the Letter is organized as follows. We begin by studying certain limiting cases, which verify the correctness of our choice (1) of the coefficient c. We then explain how our theory can be used to calculate $\varepsilon(n)$ at all $r_s \ll 1$. We proceed to the study of the large-r_s Wigner

crystal where the mapping onto the contact-interaction model is no longer valid. We show that the exact asymptotics of $\varepsilon(n)$ in the $r_s \gg 1$ limit can nevertheless be derived while at $r_s \sim 1$ a simple variational approximation can be used. We also present a numerical scheme that unifies all the asymptotical formulas we obtain. It yields a seamless interpolation over the entire range of n even for $\mathcal{L} \sim 2$–3. We take it as evidence that our theory remains numerically accurate even for modestly thin wires, which may stimulate its use in practical DFT calculations. (Achieving large $\mathcal{L}$ is feasible [8] but technically difficult.)

Definitions.—We do the usual subtraction of the Hartree term in the definition of the energy density, $\varepsilon(n) \equiv L^{-1}[\langle H\rangle - \tilde{U}(0)n^2/2]$, where L is the length of the wire, H is the Hamiltonian, and the tilde denotes the Fourier transform. We further define the correlation energy density $\varepsilon_{\rm cor}$ as the difference between ε and the sum of the kinetic ε_0 and the exchange ε_x energies of the Fermi gas,

$$\varepsilon_0 = \frac{\pi^2}{6}\frac{\hbar^2}{m}\frac{n^3}{N^2}, \qquad \varepsilon_x \simeq -\frac{e^2}{\kappa}\frac{n^2}{N}\left(\ln\frac{N}{Rn} + A_T\right), \quad (2)$$

where $A_T = \frac{3}{2} - \gamma - \ln\pi \approx -0.222$, and γ is Euler constant [9].

The relations among $\varepsilon_{\rm cor}(n)$, $h(x)$, and the dielectric function $\epsilon(q, \omega)$ are (see, e.g., Ref. [10], Secs. 5.4 and 5.6)

$$\varepsilon_{xc} \equiv \varepsilon_x + \varepsilon_{\rm cor} = n^3\int_0^{r_s}\frac{dr_s}{r_s}\frac{\varepsilon_{\rm int}(n, r_s, N)}{n^3}, \quad (3)$$

$$\varepsilon_{\rm int} = n^2\int_0^\infty dx U(x)h(x), \quad (4)$$

$$\tilde{h}(q) = -1 - \frac{\hbar}{n\tilde{U}(q)}\int_0^\infty\frac{d\omega}{\pi}\,{\rm Im}\left[\frac{1}{\epsilon(q,\omega)}\right]. \quad (5)$$

RPA regime.—The validity of our mapping between the Coulomb and the contact interactions can be verified by an independent method if the limit of large N (actually, large N^2) is taken. We discuss it because it is not only an instructive example but also the case relevant for CN, where $N^2 = 16$. For large N, $\epsilon(q, \omega)$ is dominated by the random-phase approximation (RPA) [10], which sums order by order the diagrams with the largest number of fermion loops. For $q \gg k_F = \pi n/N$ the result is

$$\epsilon(q,\omega) = 1 + \frac{2nE(q)\tilde{U}(q)}{E^2(q) - (\hbar\omega + i0)^2}, \quad E(q) = \frac{\hbar^2q^2}{2m}. \quad (6)$$

Combined with Eq. (5), it entails that at $\mathcal{L} \ll na_B \ll N^2\mathcal{L}$ (the RPA regime), the XCH has the depth $|h(0)| \simeq (\pi n l_*)^{-1}$ and a characteristic width

$$l_* = \sqrt{a_B/2n\ln(l_*/R)}. \quad (7)$$

The XCH is much deeper than in the Fermi gas, $|h(0)| \gg 1/N$, and so the correlations are strong; yet $|h(0)| \ll 1$, so that the RPA is still reliable. From Eq. (4) we find, to the leading order in $1/N$,

$$\varepsilon_{xc} \simeq -\frac{2}{3\pi}\frac{e^2}{\kappa a_B^2}\left\{\frac{1}{r_s}\left[\ln\left(\frac{l_*}{R}\right) - \frac{1}{2}\right]\right\}^{3/2}. \quad (8)$$

Repeating the same calculation for the contact interaction with c given by Eq. (1), we obtain *exactly the same* result. To track down how this comes about, it is convenient to do the integration in Eq. (4) in the q space. The interaction potential enters through its Fourier transform $\tilde{U}(q) \simeq (2e^2/\kappa)\ln(1/qR)$, which is a slow function of q. The integral is dominated by $q \sim 1/l_*$, and so to the leading order in $\mathcal{L}^{-1}$, $\tilde{U}(q)$ can be replaced by the $\tilde{U}(1/l_*)$, i.e., $U(x) \to (\hbar^2c/m)\delta(x)$, as we claimed above.

The RPA eventually breaks down at small n, where it predicts $h(0)$ to drop below the strict lower bound of -1 required by the non-negativity of the electron density. This places the lower boundary of the RPA regime at $n \sim \mathcal{L}/\pi a_B$. What happens at lower n is discussed next.

CTG regime.—The case of $n \ll \mathcal{L}/a_B$ has, in fact, already been studied in Ref. [8]. We showed that at such n electrons should form a correlated state of the Coulomb Tonks Gas (CTG). The CTG can be defined as the state where on short length scales electrons behave as impenetrable but otherwise free. It owes its name to a certain similarity it enjoys with the Tonks-Girardeau gas of 1D cold atoms [11]. It is worth mentioning that the long-distance behavior in the RPA, CTG, and Wigner crystal regimes is universally the same and is described by the LL theory. In the limit $R \to +0$, i.e., $c, \mathcal{L} \to \infty$, the ground-state wave function Ψ factorizes into the isospin part Φ and the orbital part (the remainder) [8]:

$$\Psi = \Phi \times e^W(-1)^Q\prod_{Qi>Qj}\left[\sin\frac{\pi}{L}(x_{Qi} - x_{Qj})\right]^\lambda, \quad (9)$$

where $Q1$ through QM are the indices in the spatially ordered list of the electron coordinates $0 < x_{Q1} < \cdots < x_{QM} < L$ (periodic boundary conditions are assumed), $(-1)^Q$ is the parity of the corresponding permutation, and $\lambda = 1$ for now. For $N = 2$, Φ coincides with the ground state of a spin-1/2 Heisenberg chain; for $N > 2$, see Ref. [12]. We do not discuss the function W here because it has negligible effect on $h(x)$ for $x \ll a\exp(1/r_s)$ [8]. Once W is set to zero, Ψ becomes the ground state of the contact-interaction problem at $c = \infty$ (the gas of impenetrable fermions) [13,14]. This is another explicit demonstration of our mapping, this time in the $\mathcal{L} \to \infty$ limit. Note that the XCH has the largest possible depth of unity and the width $l_* = a$.

For a finite R, Ψ remains the correct approximation to the ground state to the leading order in $\mathcal{L}^{-1}, r_s \ll 1$. We use Ψ (with $W = 0$) as a trial state to evaluate $\varepsilon(n)$. Independent of the form of Φ, the result is given by Eq. (2) with $N = 1$ (see also Ref. [8]),

$$\varepsilon(n) = \frac{e^2}{\kappa}n^2[\ln(Rn) - A_T] + \frac{\pi^2}{6}\frac{\hbar^2}{m}n^3, \quad (10)$$

which agrees with $\varepsilon(n)$ for the contact-interaction problem

to the order $1/\mathcal{L}$ [Eq. (15)], validating our mapping once again.

Bethe ansatz.—The most remarkable consequence of the mapping between the Coulomb and the contact-interaction models is that a unified treatment of all $r_s \ll 1$ regimes is possible. This is due to the fact that the latter model is solvable by the Bethe ansatz [15]. The exact energy density at any given n is given by [14]

$$\varepsilon(n) = -\frac{\hbar^2}{2m} cn^2 + \frac{\hbar^2}{2m} \int_{-Q}^{Q} dk k^2 \rho(k), \tag{11}$$

where $\rho(k)$ is the solution of the integral equation

$$\frac{1}{2\pi} = \rho(k) - \int_{-Q}^{Q} dk' G(k-k')\rho(k'), \tag{12}$$

$$G(k) = \frac{1}{\pi c N} \mathrm{Re}\left[\psi\left(1 + \frac{ik}{Nc}\right) - \psi\left(\frac{ik+c}{Nc}\right)\right]. \tag{13}$$

Here $\psi(z)$ is the digamma function [9] and $Q = Q(n)$ is fixed by the constraint $n = \int_{-Q}^{Q} dk \rho(k)$. Two analytical asymptotics of the solution can be obtained [14,16]

$$\varepsilon \simeq \frac{\hbar^2}{m}\left[-\frac{2}{3\pi}(cn)^{3/2} + \frac{\pi^2}{6}\frac{n^3}{N^2}\right], \quad c \ll n \ll cN^2, \tag{14}$$

$$\simeq \frac{\hbar^2}{m}\left[-\frac{1}{2}cn^2 + \frac{\pi^2}{6}n^3\right], \qquad n \ll c, \tag{15}$$

in agreement with Eqs. (8) and (10). From the theory point of view, Eqs. (1), (7), and (10)–(13) solve the problem of computing $\varepsilon(n)$ at all $r_s \ll 1$. A *practical* algorithm for finding the solution is given shortly below.

Wigner crystal.—At very low densities, $r_s \gg 1$, the mapping onto the contact-interaction problem is, however, *invalid.* The tails of the Coulomb barriers that separate nearby electrons are strong enough to keep them at almost equidistant positions (although the long-range order is eventually destroyed by fluctuations). According to the standard strong-coupling perturbation theory, the ground-state energy in this regime is equal to the Madelung sum plus the zero-point phonon energy,

$$\varepsilon = \frac{e^2}{\kappa} n^2 [\ln(Rn) - A_W] + C_{\mathrm{ph}} \frac{e^2}{\kappa} n^{5/2} a_B^{1/2}, \tag{16}$$

where $A_W = \ln 2 - \gamma \approx 0.116$ and $C_{\mathrm{ph}} \approx 1.018$. As for the cluster function $h(x)$, it can be obtained by interpolating between the collective phononlike correlations at $x \gtrsim a$ and two-body correlations at $x \ll a$ (see, e.g., Ref. [17]).

Variational and numerical interpolation.—Until now we expanded on a formalism that gives results both for $\varepsilon(n)$ and for $h(x)$ that are rigorously correct to the leading order in a suitable small parameter, either $1/\mathcal{L}$ or $1/r_s$. These results, e.g., the functional form of $\varepsilon(n)$ in various regimes [Fig. 1(a)], have an academic or methodological interest. In the remainder of this Letter we shift the focus to a more pragmatic goal. We wish to find a computational scheme that gives an accurate *numerical* approximation to the same quantities when neither $\mathcal{L}$ nor r_s are truly large. We achieve this by combining a variational method with a numerical interpolation. Some results are shown in Figs. 1(b) and 1(c). The concrete interpolation scheme used in generating these plots is as follows. For $r_s \lesssim 2$, $\varepsilon(n)$ is calculated by numerically solving Eqs. (1) and (11)–(13) with $l_* = \pi \exp(A_T)/Q(n, c)$. Note that function $Q(n)$ has the following limiting forms: $Q \simeq \pi n$ for $n \ll c$, $Q \simeq 2\sqrt{nc}$ for $c \ll n \ll cN^2$, and $Q = \pi n/N$ for $n \gg cN^2$. This entails that our choice of l_* is exact at small and large n, and is adequate everywhere in between; see Eqs. (2), (7), and (10).

All that remains is to handle the $r_s \gtrsim 2$ regime where the crossover between the CTG and the Wigner crystal occurs. Our solution is to treat λ in Eq. (9) as a variational parameter. This ensures a smooth transition from the CTG ($\lambda = 1$) to the Wigner crystal ($\lambda \gg 1$), provides a strict upper bound on $\varepsilon(n)$, and can be done semianalytically. Indeed, the energy density of the state $\Psi(\lambda)$ is the sum of the kinetic $\varepsilon_{\mathrm{kin}}^{\mathrm{var}}$ and the potential $\varepsilon_{\mathrm{int}}^{\mathrm{var}}$ terms. By virtue of a formula similar to Eq. (3), $\varepsilon_{\mathrm{kin}}^{\mathrm{var}}$ can be computed differentiating the known energy density $\varepsilon_{\mathrm{CS}}(\lambda)$ in the Calogero-Sutherland model [18] with respect to its coupling constant $c = \lambda(\lambda - 1)$,

$$\varepsilon_{\mathrm{kin}}^{\mathrm{var}} = \left(1 - c\frac{\partial}{\partial c}\right)\varepsilon_{\mathrm{CS}} = \frac{\pi^2}{6}\frac{\hbar^2 n^3}{m}\frac{\lambda^3}{2\lambda - 1}. \tag{17}$$

To get $\varepsilon_{\mathrm{int}}^{\mathrm{var}}$, we calculate it at $\lambda = \frac{1}{2}, 1, 2$, and ∞ using the exact cluster functions $h(x)$ [19] and interpolate between the obtained four values by a cubic polynomial in λ^{-1},

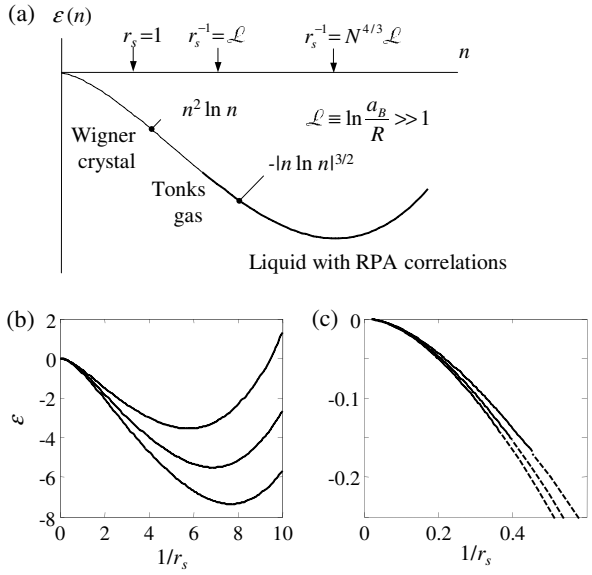

FIG. 1. (a) Qualitative behavior of $\varepsilon(n)$. (b) ε in units of $e^2/\kappa a_B^2$ for $a_B/R = 10, 15, 20$ (top to bottom), evaluated numerically. (c) The low-density part of the same plot; solid lines are from the variational method, and the dashed lines are from the Bethe ansatz.

$\varepsilon_{\rm int}^{\rm var} = (e^2/\kappa)n^2[\ln(Rn) - A_W - a_1\lambda^{-1} - a_2\lambda^{-2} - a_3\lambda^{-3}]$. For example, in the $\mathcal{L} \to \infty$ limit we find $a_1 \approx -0.3173$, $a_2 \approx -0.02363$, and $a_3 \approx 0.003\,048$. The smallness of a_2 and a_3 implies a high numerical accuracy of this polynomial fit. Minimizing $\varepsilon_{\rm kin}^{\rm var} + \varepsilon_{\rm int}^{\rm var}$ with respect to λ (numerically), we get $\varepsilon(n)$. The quality of our variational method can be judged by how well it compares with Eq. (16) in the $r_s \gg 1$ limit. It is easy to see that the functional form of $\varepsilon(n)$ is reproduced correctly, but the coefficient in front of the phonon term is approximately 1.022, i.e., higher than $C_{\rm ph}$ by a mere 0.4%. The results of this procedure, implemented for several values of a_B/R, are plotted in Figs. 1(b) and 1(c) The curves produced by the Bethe ansatz and the variational method match virtually seamlessly. Thus, the proposed scheme gives a theoretically well-founded and numerically accurate DFT needed in applications, some of which are discussed next.

Implications.—The main physical omission of our theoretical model is the screening of Coulomb interactions by other 1D subbands that may be present in a wire. Such a screening is averted if κ exceeds a certain threshold $\kappa_{\rm th}$. For CN, we estimate $\kappa_{\rm th} \sim N\mathcal{L}$, e.g., $\kappa_{\rm th} \sim 12$ for $N = 4$ and $\mathcal{L} = 3$. Note that κ is equal to the dielectric constant κ_0 of the medium if the nanotube is immersed in it and is equal to $(\kappa_0 + 1)/2$ if the medium is used as a substrate. If $\kappa < \kappa_{\rm th}$, our theory can still apply at sufficiently low n, e.g., in the Wigner crystal regime.

One possible application of our results for $\varepsilon(n)$ is a fine-tuning of the operational parameters of carbon nanoelectronic devices [4,5]. On a crude level, such devices are tiny capacitors made of CN and control metallic gates. Precise knowledge of their capacitance per unit length C is desirable for their optimal design and efficiency. The quantum and many-body effects influence the measured value of C according to the equation (see, e.g., Ref. [20])

$$C^{-1} = C_0^{-1} + (\kappa/e^2)\chi^{-1}, \qquad \chi^{-1} = \partial^2\varepsilon/\partial n^2, \quad (18)$$

where $C_0^{-1} \sim (2/\kappa)\ln(2D/R)$ is the inverse classical (geometric) capacitance and χ^{-1} is the inverse thermodynamic density of states (ITDOS). The quantum correction due to the ITDOS may be non-negligible if the distance D between the CN and the gate is small or if n is low, so that $D \sim a$. The measurable signature of a finite χ^{-1} would be the n dependence of C. Recently, the capacitance of CN and their junctions was studied in Ref. [20] by a 3D DFT. It would be interesting to apply our theory to the same structures for comparison.

The sign of the ITDOS is determined by the convexity of the $\varepsilon(n)$ curve. From Fig. 1 we see that at low enough electron densities ITDOS becomes negative. This phenomenon is a generic feature of a strongly correlated electron matter [21]. Unlike the case of neutral systems, here the negative ITDOS does not imply any thermodynamic instability but leads instead to a small *overscreening* of an external electric charge. One possible technique to detect such an overscreening experimentally is the scanned probe imaging of the electrostatic potential along an ultrathin wire (e.g., the CN [22]) set on a dielectric substrate. Above the puddles of the electron liquid induced by stray random charges, one would see the potential of a "wrong" curvature: higher near the center of the puddle, lower near its ends. The puddles can be intentionally created by additional small gates.

Finally, from $\varepsilon(n)$ one can extract the n dependence of the LL parameters that influence charge tunneling and low-temperature transport in 1D wires. Preliminary results and their comparison with other work in the literature [23] have been reported in Ref. [8]. A more detailed investigation that incorporates the results derived in this Letter will be presented elsewhere [16].

This work was initiated at MIT and completed at UCSD. The support from MIT Pappalardo Program, Sloan Foundation, and C.&W. Hellman Fund is gratefully acknowledged. I thank L. Levitov for important contributions to this project and also D. Arovas and E. Pivovarov for discussions.

[1] R. Saito, G. Dresselhaus, and M. S. Dresselhaus, *Physical Properties of Carbon Nanotubes* (Imperial College Press, London, 1998).
[2] Y. Huang *et al.*, Science **294**, 1313 (2001).
[3] A. Nitzan and M. A. Ratner, Science **300**, 1384 (2003).
[4] S. J. Tans, A. R. M. Verschueren, and C. Dekker, Nature (London) **393**, 49 (1998); R. Martel *et al.*, Appl. Phys. Lett. **73**, 2447 (1998).
[5] A. Javey *et al.*, Nat. Mater. **1**, 241 (2002); B. M. Kim *et al.*, Appl. Phys. Lett. **84**, 1946 (2004).
[6] F. D. M. Haldane, J. Phys. C **14**, 2585 (1981).
[7] H. J. Schulz, Phys. Rev. Lett. **71**, 1864 (1993).
[8] M. M. Fogler, cond-mat/0408079.
[9] I. S. Gradshteyn and I. M. Ryzhik, *Table of Integrals, Series, and Products*, edited by A. Jeffrey and D. Zwillinger (Academic Press, San Diego, 2000), 6th ed.
[10] G. D. Mahan, *Many-Particle Physics* (Plenum, New York, 1990).
[11] T. Kinoshita, T. Wenger, and D. S. Weiss, Science **305**, 1125 (2004), and references therein.
[12] B. Sutherland, Phys. Rev. B **12**, 3795 (1975).
[13] M. Ogata and H. Shiba, Phys. Rev. B **41**, 2326 (1990).
[14] P. Schlottmann, Int. J. Mod. Phys. B **11**, 355 (1997).
[15] C. N. Yang, Phys. Rev. Lett. **19**, 1312 (1967); B. Sutherland, Phys. Rev. Lett. **20**, 98 (1968).
[16] M. M. Fogler (unpublished).
[17] X. Zhu and S. G. Louie, Phys. Rev. B **52**, 5863 (1996).
[18] B. Sutherland, Phys. Rev. A **4**, 2019 (1971).
[19] M. L. Mehta, *Random Matrices* (Academic Press, San Diego, 1991), 2nd ed.
[20] P. Pomorski, L. Pastewka, C. Roland, H. Guo, and J. Wang, Phys. Rev. B **69**, 115418 (2004).
[21] O. V. Dolgov, D. A. Kirzhnits, and E. G. Maksimov, Rev. Mod. Phys. **53**, 81 (1981).
[22] A. Bachtold *et al.*, Phys. Rev. Lett. **84**, 6082 (2000).
[23] W. Hausler, L. Kecke, and A. H. MacDonald, Phys. Rev. B **65**, 085104 (2002), and references therein.